Review

Progress on Designing Artificial Solid Electrolyte Interphases for Dendrite Free Sodium Metal Anodes

Pengcheng Shi [#] , Xu Wang [#] , Xiaolong Cheng , Yu Jiang [*]

Posted Date: 23 May 2023

doi: 10.20944/preprints202305.1544.v1

Keywords: Sodium metal; artificial SEI; dendrite formation; batteries

Review

Progress on Designing Artificial Solid Electrolyte Interphases for Dendrite Free Sodium Metal Anodes

Pengcheng Shi [1,#], Xu Wang [2,#], Xiaolong Cheng [1] and Yu Jiang [1,*]

[1] School of Materials Science and Engineering, Anhui University, Hefei, 230601, China
[2] School of Computer Science and Engineering, Anhui University of Science and Technology, Huainan, 232001, China
* Correspondence: Correspondence: jiangyu21@ahu.edu.cn
# These authors contributed equally as co-first author.

Abstract: The nature abundant sodium metal is proposed as ideal anode materials for advanced batteries due to its high specific capacity of 1166mAh g^{-1} and low redox potential of -2.71V. However, the uncontrollable dendritic Na formation and low coulombic efficiency are still major obstacles for applications. Notably, the unstable and inhomogeneous solid electrolyte interphase (SEI) is recognized to be the root cause. As SEI layer plays a critical role in regulating uniform Na deposition and improving cycling stability, researches on SEI modification, especially the artificial SEI modifications has been extensively investigated recently. In this regard, we discussed the advances on artificial interface engineering from the aspects of inorganic, organic and hybrid inorganic/organic protective layers. Finally, we also highlighted the conclusions and key prospects for further investigations. We hope this review can provide a new insight for sodium metal protection.

Keywords: sodium metal; artificial SEI; dendrite formation; batteries

1. Introduction

To date, the sodium (Na) ion batteries have been commercialized as a supplement technology for lithium (Li) ion batteries due to the natural abundant Na resources and low price [1]. However, the energy density of Na ion batteries seems to be unsatisfied as compared with update commercial Li ion batteries [2, 3]. To meet the rapidly growing demand markets on energy density of Na ion batteries, the development on advanced electrode materials with high capacity are highly desired [4].

Among various materials, the metal Na has been proposed as an ideal candidate due to its high specific capacity (1166mAh g^{-1}) and low redox potential (-2.71V) [5-7]. In this regard, the investigations on metal Na based batteries such as Na-S; Na-O_2 and Na-CO_2 batteries have also been widely reported [5]. However, the cycling performances and safety issue of Na anode are still unsatisfactory. It is explored that the ultra-high reactivity of Na in electrolyte may be the root reason. The spontaneously reaction between Na and electrolyte can form a solid electrolyte interphase (SEI) on the surface, which is proved to be chemical/mechanical unstable and fragile [8, 9]. During plating/striping, the thermodynamic SEI would be thickened, broken and collapsed. At the same time, the inhomogeneous SEI further induces uneven Na^+ flux locally, as a result of mossy/dendritic Na formation [7, 9]. Additionally, the volume change during Na plating/striping is very obvious, especially under industry conditions (more than 3.5 mAh cm^{-2} for each deposition cycle) [10]. Consequently, the thickness change can lead to great local stress, making the SEI to be much more unstable and more easily cracking [11]. The cracks then increases the local Na^+ flux around, which in turn aggravates the growth of dendritic Na. In particular, the dendritic Na can penetrate through separator and detach from the matrix easily to form "dead" Na, leading battery short circuit and short cycle life [11, 12]. This phenomenon also consumes electrolyte and active Na, as a consequence of low coulombic efficiency [13]. Therefore, effective efforts on modification Na metal anode are highly necessary.

Under this background, several approaches have been proposed to stable Na anodes. For instance, constructing 3D host to resolve infinite volume expansion [6, 14, 15]; coating separator to

Preprints (www.preprints.org) | NOT PEER-REVIEWED | Posted: 23 May 2023 doi:10.20944/preprints202305.1544.v1

block Na dendrites [16, 17] and employing Na alloy to build stable anodes [18-20]. Although these approaches have some positive effects in suppressing dendritic Na formation, the properties of SEI films are still unsatisfied and the irreversible side reactions can't be totally suppressed. The electrolyte modification seems to be promising for increasing the stability of the SEI interphase. However, the additives, salts and solvents can't hold for long-term cycling due to the continuous consumption [11, 21]. According, the ideal SEI for Na metal should possess excellent chemical/electrochemical stability, good ionic conductivity, even Na^+ flux/electric field distribution, sufficient Young's module, good flexibility, and robustness [22]. In this regard, artificial interphase engineering is of vital important since the protective layer can be precisely designed and easily adjusted. More importantly, the artificial SEI can meet most of the above mentioned merits of ideal SEI. So far, extensive researches have been proposed for artificial interphase configuration to improve the stability of SEI [23, 24]. Therefore, it is necessary to summarize the research progress on artificial SEI designing in recent years. Herein, in this review, we discussed the advances on artificial interface engineering from the aspects of inorganic, organic and hybrid inorganic/organic protective layers as shown in Figure **1**. We also conclude by prospecting future direction of artificial interphase chemistry for advanced Na metal anodes. We hope this review can deep the understanding on artificial SEI layers, thus exploring stable and dendrite free Na anodes.

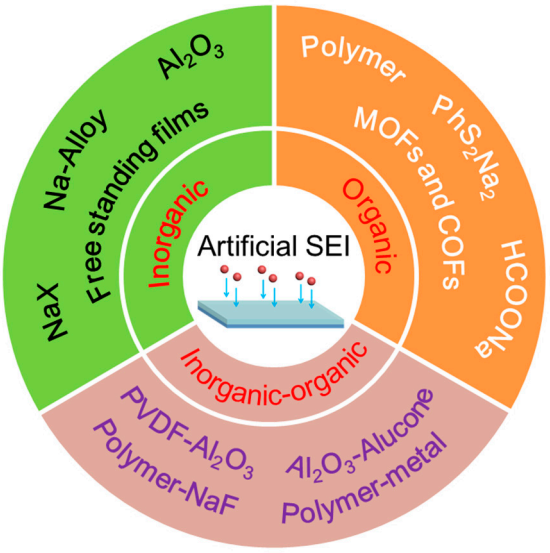

Figure 1. Schematic illustration of artificial interface engineering from the aspects of inorganic, organic and hybrid inorganic/organic protective layers.

2. Challenges for Dendrite Free Na Metal Anodes

Like other alkali metals, Na is thermodynamic unstable, which is the root cause of uncontrollable parasitic reactions and the formation of chemical/mechanicl unstable SEI [23, 24]. Figure **2** shows the main challenges of Na metal anodes. As compared with Li metal, Na metal is more prone to deposited in dendritic morphology and suffers from severer volume expansion, along with SEI breakage and low Coulombic efficiency during repeated plating/striping [25, 26]. Overall the challenges for dendrite free Na metal anodes are discussed as following.

Preprints (www.preprints.org) | NOT PEER-REVIEWED | Posted: 23 May 2023 doi:10.20944/preprints202305.1544.v1

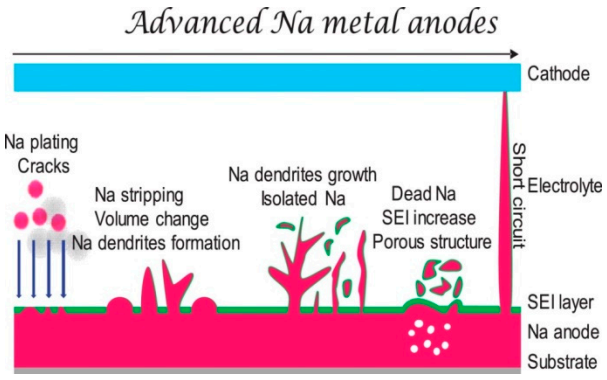

Figure 2. Schematic illustration of challenges for Na metal anodes [25]. Copyright 2018, Elsevier.

2.1. Unstable SEI

Because of the highly reactive nature and very negative voltage potential, the electrolyte can be reduced spontaneously on Na metal anode to form an SEI layer. It is expected that such a passivation layer is dense and inert so as to effectively isolate electron transfer and prevent further parasitic reactions [24, 27-29]. Nevertheless, the SEI layer is demonstrated to be structure porous and fragile in common electrolytes.

As it is recognized, the SEI layer formed on Na metal is mainly composed of inorganic species (e.g., NaF, Na_2O and Na_2CO_3) and organic species (e.g., RONa, $ROCO_2Na$, and RCOONa; where R is the alkyl group) [25]. This kind hybrid organic/inorganic SEI layer are proved to be dissolved in electrolyte more easily than those of Li [30, 31]. Due to the non-uniform distribution of SEI compositions, the SEI layer formed in common electrolytes is spatial variation in ionic conductivity, resulting in uneven distribution of Na^+ flux. Meanwhile, with a "host-less" nature of Na matrix, this SEI cracks easily during repeated Na^+ plating/striping, which then in turn accelerates dendrite growth due to increased Na^+ flux and preferential Na^+ plating around the cracks. Furthermore, the repeated breakage of SEI also leads to uncontrollable electrolyte consumption, followed by low coulombic efficiency and high SEI impedance [32, 33]. As a result, Na metal with unsatisfied SEI properties inevitably suffers from poor performances.

Based on previous understanding [34, 35], further progresses on building ideal SEI for dendrite free Na metal should be with following characteristics: firstly, highly Na^+ conductive so as to facilitate uniform Na^+ deposition and regulate preferential Na plating; secondly, electrochemically stable and electronically insulated to prevent further side reactions; thirdly, robust enough to long-time hold huge volume expansion and dendrite propagation, and finally homogeneity in composition to decentralize the Na^+ flux.

2.2. Uncontrollable Dendritic Na formation

The notorious dendrite is also a serious problem for achieving safe and stable Na anode. The dendrite growth can penetrate the separator, leading to battery short circuit and poor cycling stability. Different from conventional needle-like Li dendrites, the morphology of Na dendrites is reported to be mossy or flocculent like with severe porous structures [36, 37].

Based on previous understanding [38], it is widely accepted that the concentration of Na^+ will decrease to zero near the surface in Sand's time. Due to the spatial variation in ionic conductivity and localized electric field, the rough surface will induce uneven Na^+ plating/striping, resulting in dendrite formation. Subsequently, the tips of dendrites would be hot sites for further dendritic Na nucleation and growth due to its larger electric field and ionic concentration gradients. Once the dendrite nucleated, the growth rate of dendrites is a key parameter to determine the lifetime of Na anode. According to the Sand's law, the speed of dendrite formation is inversely proportional to square of the deposition current [32, 37, 39, 40].

Preprints (www.preprints.org) | NOT PEER-REVIEWED | Posted: 23 May 2023 doi:10.20944/preprints202305.1544.v1

The dendrite growth can expose fresh Na surface with depletion of electrolyte and active Na. Meanwhile, the structure unstable dendrites would detach from the matrix to form "dead" Na. Through microscopy observation, it is proved that the porous Na dendrites can break away from the bulk Na matrix easily, as compared with Li dendrites. The dendrites intrinsically exhibit much higher chemically reactivity and weaker mechanical stability [39].

2.3. Severe Volume Expansion

The severe volume expansion can be regard as the root cause of the continuous side reactions. Theoretically, the thickness would increase 8.86μm under 1 mAh cm^{-2} deposition of Na. To satisfy industrial requirements, the deposited capacity would be above 3.5 mAh cm^{-2} [34, 41]. Due to uneven deposition, the practical volume variation would be more obvious than theoretical expected. In addition, due to the host-less nature, the volume expansion is considered to be relatively infinite. It is recognized this volume expansion would further induce inner stress and local expansion/contraction, resulting fracture of the SEI layer and pulverization of active Na. This phenomenon in turn accelerates side reactions and dendrite growth [42]. To alleviated the volume expansion and mitigate the inner strain, nanostructured host such as Cu foam [43-45], carbon matrix [42, 46, 47] and Mxene [48, 49] are proposed to accommodate Na. Nevertheless, these host increases the total weight and volume of the Na anode at the expense of total energy density. The recent development of hosts for dendrite free Na metal has been discussed in several reviews [26, 50].

3. Advances in Artificial SEI Interphase

Stable SEI is the ultimate pursuit for achieving dendrite free Na metal anodes. With deep understanding of plating/stripping mechanism, several strategies (e.g., chemical pretreatment, building protective film by advanced deposition technologies and free-standing protective layers) for building artificial interphase have been proposed [36, 37, 39]. Typically, the chemical composition, structure, and thickness of artificial SEI layers can be precisely controlled by optimizing the reagent species, concentration and reaction temperature, time, etc [36]. As reported, the artificial SEI can be classified into inorganic rich, organic rich or their hybrids [24, 51, 52]. The characteristic of the inorganic rich and organic rich SEI are schematic presented in Figure **3**a-b. In this section, we will discuss the recent advances in constructing artificial SEI for stable Na metal anodes.

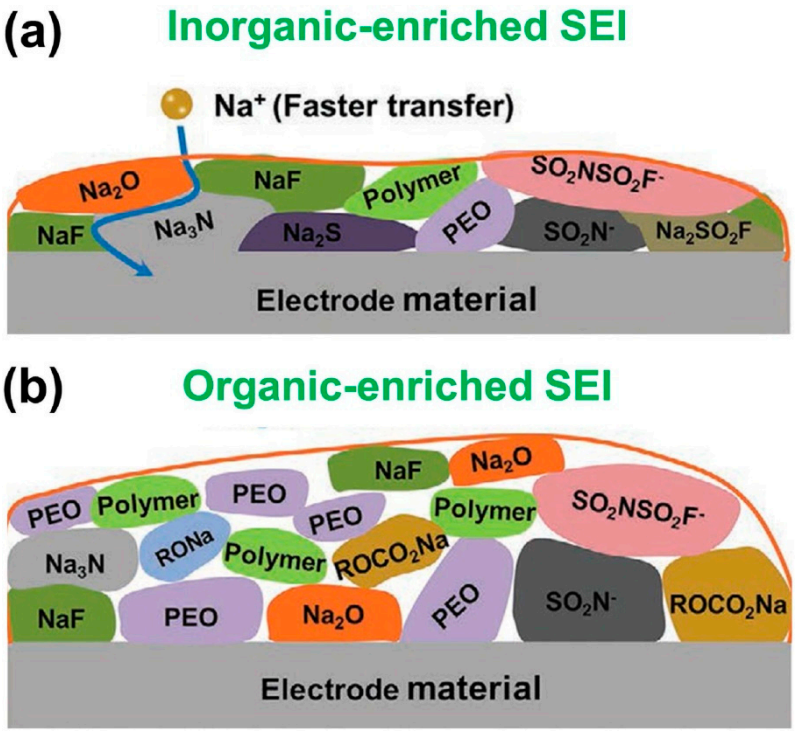

 doi:10.20944/preprints202305.1544.v1

Figure 3. Schematic illustration of (a) the inorganic-enriched SEI and (b) organic-enriched SEI on Na metal [51]. Copyright 2021, Wiely-VCH.

3.1. Inorganic Interphase

By adopt the experiences and knowledge of LiX (X=F, Cl, Br, I) for dendrite suppression in Li metal batteries, NaX are proposed for inorganic interphase configuration through chemical pretreatment methods [22, 36, 53]. In the early stage, Wang et al. proposed a facile chemical pretreatment of Na with SbF_3/DMC solution. Through an exchange reaction, an inorganic SEI rich in NaF and Na_3Sb alloy is formed. Take advantages of the synergistic effect of NaF and Na_3Sb, the hybrid NaF/Na_3Sb interphase greatly reduces the surface reactivity and interfacial impedance [54, 55]. Lately, the NaF rich interphase was also reported by reaction with 1-butyl-2,3-dimethylimidazolium tetrafluoroborate ($BdmimBF_4$) [56], CoF_2 [57], AlF_3 coated solid-state electrolyte [58] and triethylamine trihydrofluoride [59]. The role of NaF for dendrite suppression is benefit from the high shear modulus of 31.4 GPa, which is much higher than that of metal Na (3.3 GPa) [57, 60]. Inspired by these works, NaCl rich interphase is also investigated. For instance, Huang et al. adopted $SnCl_2$ to treat Na with the formation of NaCl/Na-Sn alloy interphase [61]. As expected, both rapid ion transportation and suppressed parasitic reactions is obtained, which jointly achieve a nondendritic morphology over 500h in Na||Na batteries. Similar treat methods have also been reported by $ZnCl_2$ and $SnCl_4$ [62-64]. Analogous to NaF and NaCl, the NaI and NaBr rich interphase was reported by reaction with 1-iodopropane and 1-bromopropane, respectively [65, 66]. In Na||Na cells, the NaI coated Na was stable for 500h under 0.25 mA cm^{-2}, 0.75 mAh cm^{-2}, while the NaBr coated Na was stable for 250h under 1.0 mA cm^{-2}, 1.0 mAh cm^{-2}. According to the density functional theory calculations in Figure **4**a, the energy barriers for interface ion diffusion is decreased in following order: NaF>NaCl≈NaI>NaBr [66]. The lower energy barrier is more favorable for nondendritic deposition.

The S containing protective layer is also attractive for nondendritic Na plating /stripping due to its high ionic conductivity. Sun et al. synthesized Na_3PS_4 as an artificial protective layer by reacting Na with P_4S_{16} in diethylene glycol dimethyl ether. By controlling the concentrations of P_4S_{16} and reacting time, the thickness and composition of the Na_3PS_4 can be optimized. The thin Na_3PS_4 layer can prevent unwanted side reactions and uniform the Na^+ flux during plating/striping [67]. The Mo_6S_8 and MoS_2 were also used for building $Na_xMo_6S_8$ and Na_2S protective layers as shown in Figure **4**b-c, respectively [68, 69]. Besides NaX and the S containing protective layer, the Na_3N layer is also attractive due to its high ionic conductivity. In 2021, Sun et al. directly embedded $NaNO_3$ into Na matrix with the formation of Na_3N and NaN_xO_y in Figure **4**d-e. The Na_3N and NaN_xO_y provides good SEI stability and Na^+ conductivity, while the remained $NaNO_3$ remain as a SEI stabilized for long term cycling [70].

Recently, the Yu's group built a Na_3P protective layer to stable Na metal via treating with red phosphorus. As shown in Figure **4**f, the Na_3P layer can provide high ionic conductivity of ~0.12 mS cm^{-1} and high Young's modulus of 8.6 GPa, which regulates uniform Na^+ flux and prevents the dendrite growth. As proved by cryo-TEM, the Na_3P phase can still be remained after repeated plating/striping, which is highly attractive for achieving stable Na anode. Benefiting from these advantages, the Na||Na cells with the Na_3P artificial layer present a nondendritic morphology for 780h at 1.0 mA cm^{-2}, 1.0 mAh cm^{-2}. In addition, the artificial phosphorus derived protection layer was also applied for dendrite free potassium metal with satisfied performances [71]. More recently, the Yu's group also proved that the Na_2Te artificial interfacial layer showed similar advantages [72]. At 1.0 mA cm^{-2}, 1.0 mAh cm^{-2}, the Na@Na_2Te provides excellent cyclic stability for 700h. As the interface with a single component can hardly meet all the requirements of ideal SEI, the Wu et al. and Ji et al. further developed a hybrid Na_3P/NaBr interphase with faster ionic conductivity compared with Na_3P as shown in Figure **4**g [73, 74]. The Rui et al. also adopted V_2S_3 [75], VN [13], VSe [76], VP_2 [77] and BiOCl [78] as precursors to build artificial heterogeneous interphase layer. With vanadium and Na_3Bi, a more uniform deposition of Na^+ is promoted and the better cycling performance is achieved.

Preprints (www.preprints.org) | NOT PEER-REVIEWED | Posted: 23 May 2023 doi:10.20944/preprints202305.1544.v1

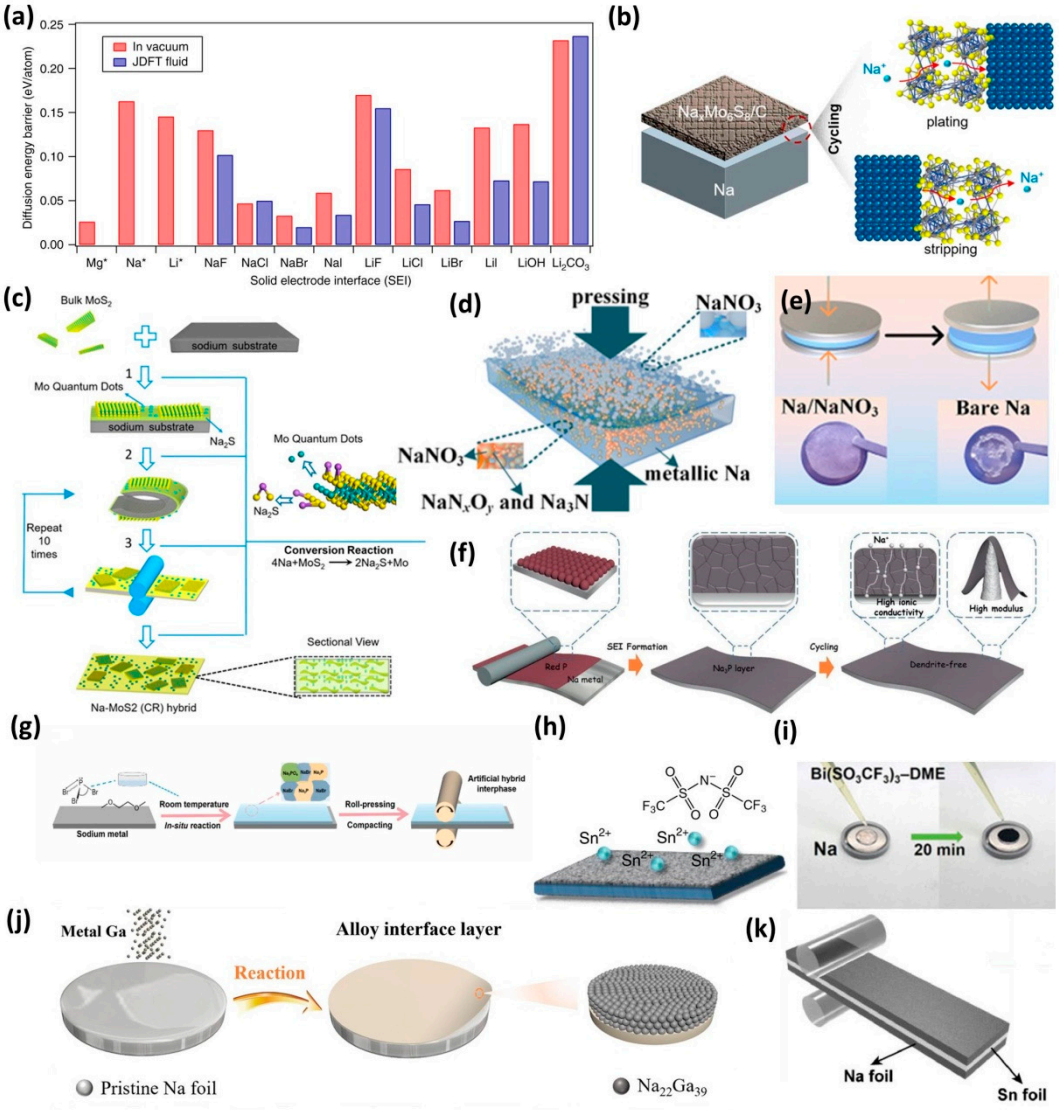

Figure 4. (a) Calculated energy barriers for Mg, Na and Li atoms diffusion on the surface with noted chemistry [66]. Copyright 2017, Nature. (b) The function of Mo_6S_8 formed $Na_xMo_6S_8$ protective layer [68]. Copyright 2019, American Chemistry Society. (c) The fabrication of Mo_2S based protective layer and the corresponding conversion reaction [69]. Copyright 2017, American Chemistry Society. (d) Mechanical fabricated $NaNO_3$ derived Na_3N/NaN_xO_y protective layer. (e) Image of the Na anodes with and without $NaNO_3$ [70]. Copyright 2021, American Chemistry Society. (f) Schematic illustration of red phosphorus formed Na_3P layer and the dendrite suppression mechanism [71]. Copyright 2021, Wiely-VCH. (g) The Na_3P/NaBr hybrid layer formed form PBr_3 [73]. Copyright 2022, Elsevier. (h) $Sn(TFSI)_2$ solution formed Na-Sn alloy protected layer [80]. Copyright 2018, Nature. (i) Photo of $Bi(SO_3CF_3)_3$ treated Na anode [81]. Copyright 2019, Wiely-VCH. Rolling of Na with (j) liquid Ga [85] and (k) Sn foil [86]. Copyright 2022, Wiely-VCH. Copyright 2021, Elsevier.

The solely Na alloy interphases are also attractive. Due to the low reduction potential of Na, the metal cations dissolved in solvents can spontaneously alloy with Na. For Li metals, Li et al. immersed Li in $Mg(TFSI)_2$ containing electrolyte with the formation of Li-Mg alloy [79]. The pre-alloying with Mg avoids the nucleation of Li at the hot points for dendrite growth and prevents the electrolyte corrosion. As similar system, this approach also apples for Na metal anodes. In Figure **4**h, by taking advantage of $Sn(TFSI)_2$, the Na-Sn alloy interphase rich in Na_9Sn_4 and $Na_{14.7}Sn_4$ can be obtained. Under 0.25 mAh cm^{-2}, the Na||Na cells can physically mitigated dendrite growth for 1700h due to its fast ion transport property. Despite surface alloy, some cations can be reduced as metals, which

 doi:10.20944/preprints202305.1544.v1

usually act as nucleation seeds for dendrite suppression [80]. As shown in Figure **4**i, Chen's group use $Bi(SO_3CF_3)_3$ to treat Na with the formation of Bi. Under 0.5 mA cm^{-2}, the Na-Bi anode can cycle for 1000h without overpotential increase [81]. Analogous AgTFSI, $AgCF_3SO_3$ were also achieved with the formation of Ag seeds [82, 83]. Notably, these species are also powerful for using as additives for electrolyte modification [39]. More recently, the Yu et al. also alloy Na surface with Ga liquid metal and Sn foil via in suit rolling as shown in Figure **4**j-k [84-86].

Despite chemical pretreatment methods for inorganic SEI configuration, the physical deposition method is also proposed. Among them, the atomic layer deposition (ALD) technology is most attractive since it has long been used for building advanced protective layers for batteries. Early in 2017, a thin Al_2O_3 protective layer was achieved on Na through low-temperature plasma-enhanced ALD as shown in Figure **5**a-b [87-89]. The low temperature ALD can avoid the melting of Na (98 ^oC) due to its low working temperature of 75 ^oC. Based on the growth rate of Al_2O_3, the thickness of 10, 25, and 50 cycles of ALD Al_2O_3 is confirmed to be 1.4, 3.5, and 7 nm, respectively. Attractively, the Al_2O_3 can convert into highly conductive $NaAlO_x$ during cycling. The Na@Al_2O_3 displayed an island-like morphology up to 500 cycles even at 3 mA cm^{-2}. Analogue to ALD, the molecular layer deposition (MLD) technology is also proposed for building hybrid inorganic/organic protective layers [90]. The MLD will be discussed in the following hybrid interphase section.

Another type inorganic SEI is designed by using prefabricated free standing films. Typically, these free standing films can improve the surface sodiophilicity with function groups. Peng et al. presented an oxygen-functionalized 3D carbon nanotube film (O_f-CNT) in Figure **5**c [91]. According to DFT calculation, the oxygen function group has strong interaction with Na^+ as shown in Figure **5**d, which provides a robust sodiophilic interphase. Benefit from the sodiophilic nature, the O_f-CNT offers preferential Na nucleation with a reduced overpotential and improve the reactions kinetics. Similar free standing films also proposed with O, N functioned 3D nanofibers (ONCNFs) [92]. Despite 3D carbon nanofibers, the 2D materials such as MXenes, graphene, silicene, germanene, phosphorene, h-BN, SnS, SnSe and g-C_3N_4 film have also attracted tremendous attentions [93-95]. In order to accelerate surface Na^+ transfer and improve the ionic conductivity of the protective layer, the introduction of defect, the increase in bond length, the proximity effect should be serious considered as confirmed by first principles calculations. Meanwhile, their balance with surface stiffness against dendrite suppression is also a critical factor. In this regard, Chen et al. used MXene and carbon nanotubes (CNTs) to construct a 3D MXene/CNTs sodiumphilic layer for rapid Na^+ diffusion and dendrite suppression [96]. Li et al. also prepared Sn^{2+} pillared Ti_3C_2 MXene [97]. The Sn^{2+} can act as sodiophilic seeds and form highly conductivity $Na_{15}Sn_4$ alloy to balance the electric field. Tian et al. also reported Mg^{2+} decorated Ti_3C_2 MXene as protective layer for Na metal [98]. In addition to these, Wang et al. prepared 3D sodiophilic Ti_3C_2 MXene@g-C_3N_4 hetero-interphase in Figure **5**e, in which MXene act as the highly conductive substrate and the g-C_3N_4 act as an interfacial modulation layer to regulate Na^+ deposition. As shown in Figure **5**f, the Ti_3C_2 MXene@g-C_3N_4 hetero-interphase show largest adsorption energy, contributing to form sodiophilic surface [99]. In conclusion, these freestanding protective layers possess tuned electronic properties, strong sodiophilicity and structural robustness.

Preprints (www.preprints.org) | NOT PEER-REVIEWED | Posted: 23 May 2023 doi:10.20944/preprints202305.1544.v1

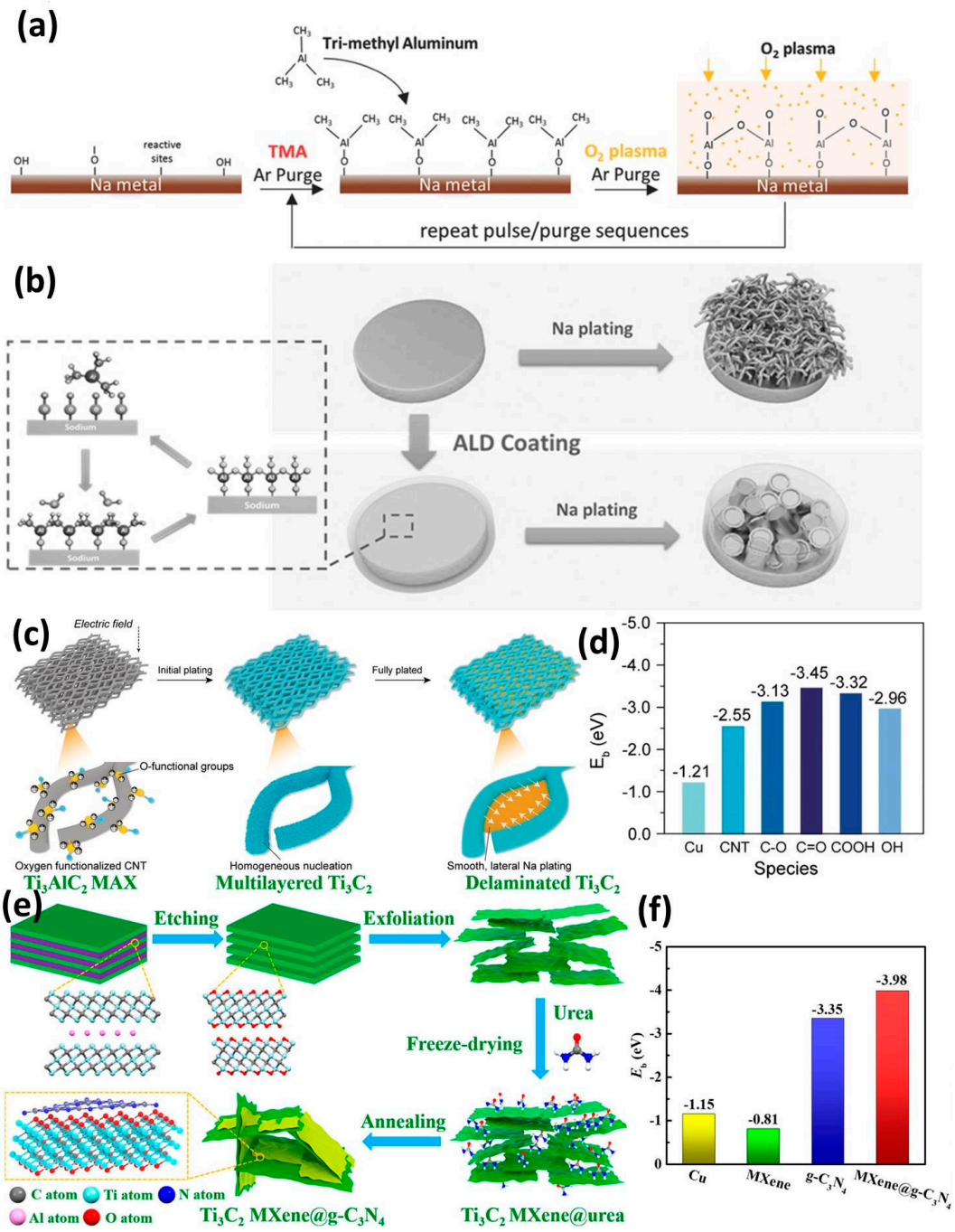

Figure 5. (a) Schematic of the ALD deposition of Al_2O_3 with TMA and O_2 plasma [87]. Copyright 2017, Wiely-VCH. (b) Plating of Na without and with ALD deposited Al_2O_3 layer [88]. Copyright 2017, Wiely-VCH. (c) Function of Of-CNT network on homogeneous nucleation and smooth Na deposition. (d) Binding energies of Na with various function groups [91]. Copyright 2019, Wiely-VCH. (e) Fabrication process of Ti_3C_2 MXene@g-C_3N_4 hetero-interphase for dendrite suppression. (f) Binding energies of Na with Cu, Ti_3C_2 MXene, g-C_3N_4 and Ti_3C_2 MXene@g-C_3N_4, respectively [99]. Copyright 2022, American Chemistry Society.

3.2. Organic Interphase

Apart from the inorganic interphase, organic interphase is also attractive since the precursor can be precisely designed and optimized from molecular level [24, 100]. The organic SEI layer is capable of alleviating the volume expansion and preventing dendrite growth due to its excellent flexibility.

Preprints (www.preprints.org) | NOT PEER-REVIEWED | Posted: 23 May 2023 doi:10.20944/preprints202305.1544.v1

Previously, the polar polymers (poly(dimethylsiloxane)(PDMS), polyacrylic acid(PAA), etc.) were proved to be strongly interacted with Li^+, which would be effective for regulating uniform distribution of ion flux [102-104]. Inspired by these works, Ma's group prepared a fibrillar poly(1,1-difluoroethylene) (PVDF) fiber film (f-PVDF) with non-through pores by electro-spun. By working as a blocking interlayer for dendrite suppression, the f-PVDF film is superior to the conventional compact PVDF film, PVDF film with through pores, polyethylene oxide (PEO), and polytetrafluoroethylene (PTFE) film. It is noticed that the polar C-F group affinity to Na^+ more stronger than C-O groups in PEO, which provides a better environment for uniform Na^+ deposition. Meanwhile, the f-PVDF show better electrolyte uptake for faster ion conductivity. More recently, Lu et al. protected Na metal anode by soaking in 1,3-dioxolane (DOL) in Figure **6**a. The polar C-O of DOL can break with the formation of poly(DOL), which enables a faster interfacial transport and a lower interfacial resistance. In detail, the polymerization of DOL forms Na alkoxides ($CH_3OCH_2CH_2ONa$ and $CH_3CH_2OCH_2ONa$) and HCOONa. Then the Na alkoxides transformed into RONa by further reacting with Na. Finally, the RONa and HCOONa in turn reacting with DOL continuously. With protected poly(DOL), a cycling life over 2800h at 1mA cm^{-2} can be obtained in symmetric cells. Attractively, Lu et al. also proposed spraying DOL for large scale manufacturing [105]. Meanwhile, as shown in Figure **6**b, Wei et. al also using imidazolium ionic liquid monomers to prepare ionic membrane through in suit electro-polymerization. The obtained ionic membrane (about 50 nm thick) can regulate the electric filed and stable Na anode [106].

Despite polymer based SEI, the organic Na benzenedithiolate (PhS_2Na_2) and HCOONa were also reported as shown in Figure **6**c-d. In 2020, Wu et al. reported a PhS_2Na_2-rich protection layer for Na metal. They first chemical treat Na metal with S_8 and para-dichlorobenzene (p-DB) in tetrahydrofuran solution, along with the formation of poly(phenylene sulfides) (PPS), NaCl, and Na_2S_y. Then it was converted into PhS_2Na_2 upon cycling. By DFT calculations, they concluded that the function of PhS_2Na_2 species. Since the binding energy of Na^+ in PhS_2Na_2 (-2.3eV), Ph-S-Na (-2.13eV) are much lower than that of CH_3ONa (-2.49eV), CH_3OCO_2Na (-2.497eV), and Na_2CO_3 (-3.5eV), a higher ionic conductivity is proved in the PhS_2Na_2 based SEI [107]. More recently, Zheng et al. treated Na with formic acid vapor via a solid-gas reaction strategy. After 10s, the original silvery white Na surface turned into dark red HCOONa, as confirmed by X-ray diffraction and Raman. Then the organic HCOONa layer can work as a robust interfacial layer with low Na^+ diffusion barrier. Additionally, the HCOONa interface can also extend to anode free batteries with format modified collectors [108].

Recently, metal-organic frameworks (MOFs) and covalent organic frameworks (COFs) have been reported to sever as ionic sieves to control uniform Na^+ plating. In 2019, the Chen et al. prepared MOF-199 and ZIF-8 as a coating layer on Cu substrate [109]. By acting as a compact and robust shield, the MOF-199 layer can physically prevent dendrite growth, thus regulating dense Na deposition and less excess SEI formation in Figure **6**e. Similar Mg based MOF-74 has also been proposed by Yang et al. They first prove that the main group II metal (Be, Mg, and Ba) can act as nucleation seeds for homogeneous Na deposition. Benefit from these merits, the Mg-based MOF-74 was used to control Na deposition. With eliminated nucleation barriers, a uniform morphology can be obtained [110]. The liquid MOFs of ZIF-62 and have also been proposed to building protective layers for solid batteries [111]. The ZIF-62 interlayer is synthesized from high-temperature monophasic of liquid MOFs. The uniform ZIF-62 layer can increase interfacial sodiophilicity and improve e^-/Na^+ transport kinetics. More recently, the sp^2 carbon COF (sp2c-COF) functioned separator is also built to induce a robust SEI in Figure **6**f [16]. The high-polarity architecture shows a good affinity toward Na^+, which helps to achieve a uniform ion flux and a nondendritic morphology during plating/stripping [112, 113]. So far, reports on applying MOFs and COFs to preventing dendrite growth of Na metal are still limit.

Preprints (www.preprints.org) | NOT PEER-REVIEWED | Posted: 23 May 2023 doi:10.20944/preprints202305.1544.v1

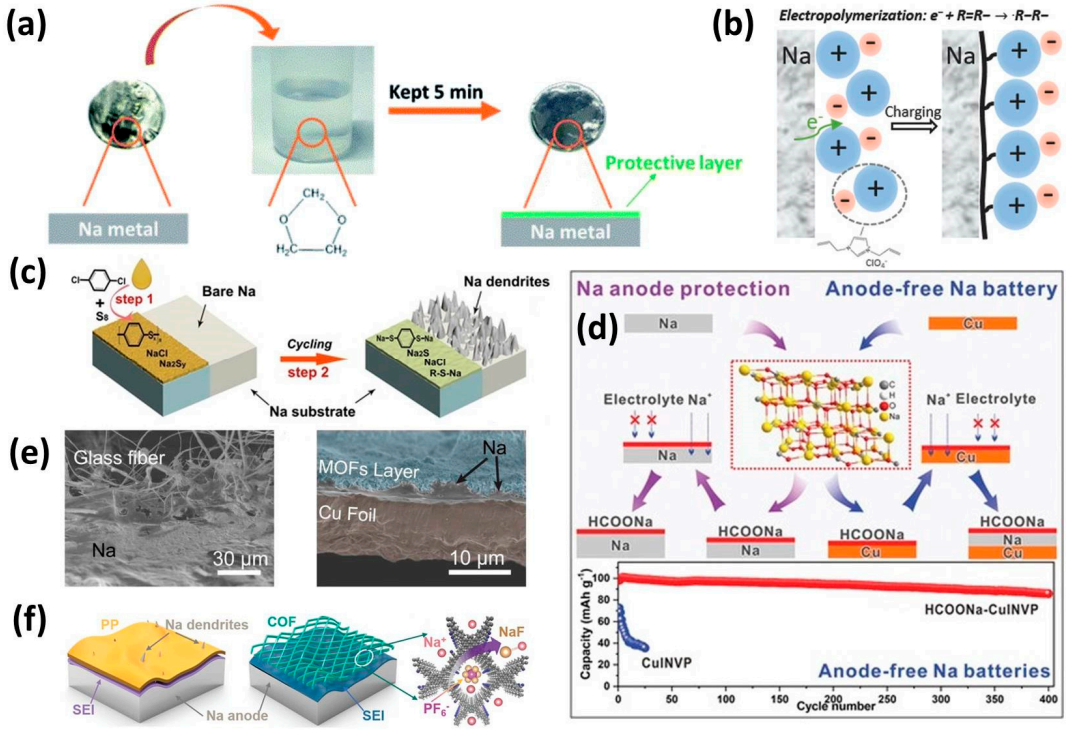

Figure 6. (a) Process of preparing poly(DOL) protected Na metal [105]. Copyright 2021, Royal Society of Chemistry. (b) In suit polymerization of imidazolium ionic liquid monomers on Na [106]. Copyright 2017, Wiely-VCH. (c) The fabrication of PhS_2Na_2-rich protection layer on Na [107]. Copyright 2019, Wiely-VCH. (d) The HCOONa protective layer on Na metal and Cu foil for Na||$Na_3V_2(PO_4)_3$ and HCOONa-Cu|| $Na_3V_2(PO_4)_3$ batteries [108]. Copyright 2023, Wiely-VCH. (e) Deposition of Na morphology on Cu foil without and with MOFs layer [109]. Copyright 2019, Elsevier. (f) Schematic illustration of COF derived artificial layer for dendrite Na suppression [16]. Copyright 2023, Wiely-VCH. .

3.3. Hybrid Interphase

To combine the advantages of artificial inorganic SEI and organic SEI, researchers have proposed hybrid organic/inorganic SEI, in which the inorganic components offers sufficient mechanical strength to suppress dendrites and the organic components gives provides a certain flexibility to alleviate the volume expansion. In 2017, Kim et al. presented a free standing inorganic/organic protective layer composed of mechanically robust Al_2O_3 and flexible PVDF polymer (FCPL). They FPCL has high shear modulus, which is critical for dendrite suppression. Nevertheless, the FCPLs with low ionic conductivity could not enhance cycling stability [114]. In order to further improve the ionic conductivity, Jiao et al. using NaF and PVDF prepared a similar free standing and implantable artificial film (FIAPL) to protect Na [115]. In FIAPL, the organic PVDF film could accommodate the volume expansion and thereby maintain the integrity of the interface, while the inorganic NaF particles can improve ionic conductivity and mechanical strength, resulting in uniform Na nucleation and deposition. The same PVDF/NaF layer was also coated on Cu substrate for Na deposition [116]. Inspired by the PVDF/NaF layer, the Yu et al. further treated Na with PTFE via in suit rolling with the formation of NaF/organic carbon species, which function with C=C and C-F groups, as shown in Figure **7**a [117]. They experimentally verified the high mechanical strength, fast ionic kinetics and good sodiophilicity of this protective layer [117-120]. As reported by Tao et al. the PTFE derived NaF/carbon layer can be rapidly induced by pressure and diglyme-induced defluorination reaction in Figure **7**b. It is explained that the diglyme can bonds with Na easily to form chains of O-Na-O, which reacting with PTFE film rapidly. Benefit from these merits, the NaF/organic carbon protective

Preprints (www.preprints.org) | NOT PEER-REVIEWED | Posted: 23 May 2023 doi:10.20944/preprints202305.1544.v1

layer shows a long life of 1800h under 3mAh cm^{-2}. They also confirmed similar H_nC-O-H_nC chain can be obtained by using other solvents [121].

The polymer/metal interphases are also proposed. In 2020, Huang et al. reported a well-designed artificial protective layer consisting of PVDF and Sn by coating on Cu collector. The PVDF film is flexible to accommodate surface expansion, whereas the sodiophilic Sn metal can offer sufficient Na^+ ions and high mechanical modulus for dendrite free plating/striping [122]. With the PVDF-Sn protective layer, a high average CE of 99.73% can be obtained for 2800h at 2 mA cm^{-2}. Li et al. also proposed a polyacrylonitrile (PAN) film with thin Sn layer coated on the down side. As shown in Figure **7**c, benefit from the low nucleation barrier of Sn seeds, the PAN-Sn protective layer can regulate Na deposition with a controlled location and orientation [123]. More recently in 2022, Li et al. constructed a similar polymer PVDF and metal Bi layer on Cu substrate (PB@Cu). The cyclic voltammetry and galvanostatic discharge curves in Figure **7**d-e confirmed the alloying/dealloying of Bi. With Bi metal, the deposition kinetics of Na is increased. At 1 mA cm^{-2} and 1 mAh cm^{-2}, the PVDF-Bi layer provides a high utilization of Na and a long life time of 2500h in Figure **7**f. The superior electrochemical performance of PVDF-Bi layer is revealed to originate from flexible PVDF, which could accommodate severe volume change induced by Na^+ plating/stripping. Meanwhile the Bi and/or sodiated Na_3Bi can offer high ionic conductivity and sufficient mechanical strength [124].

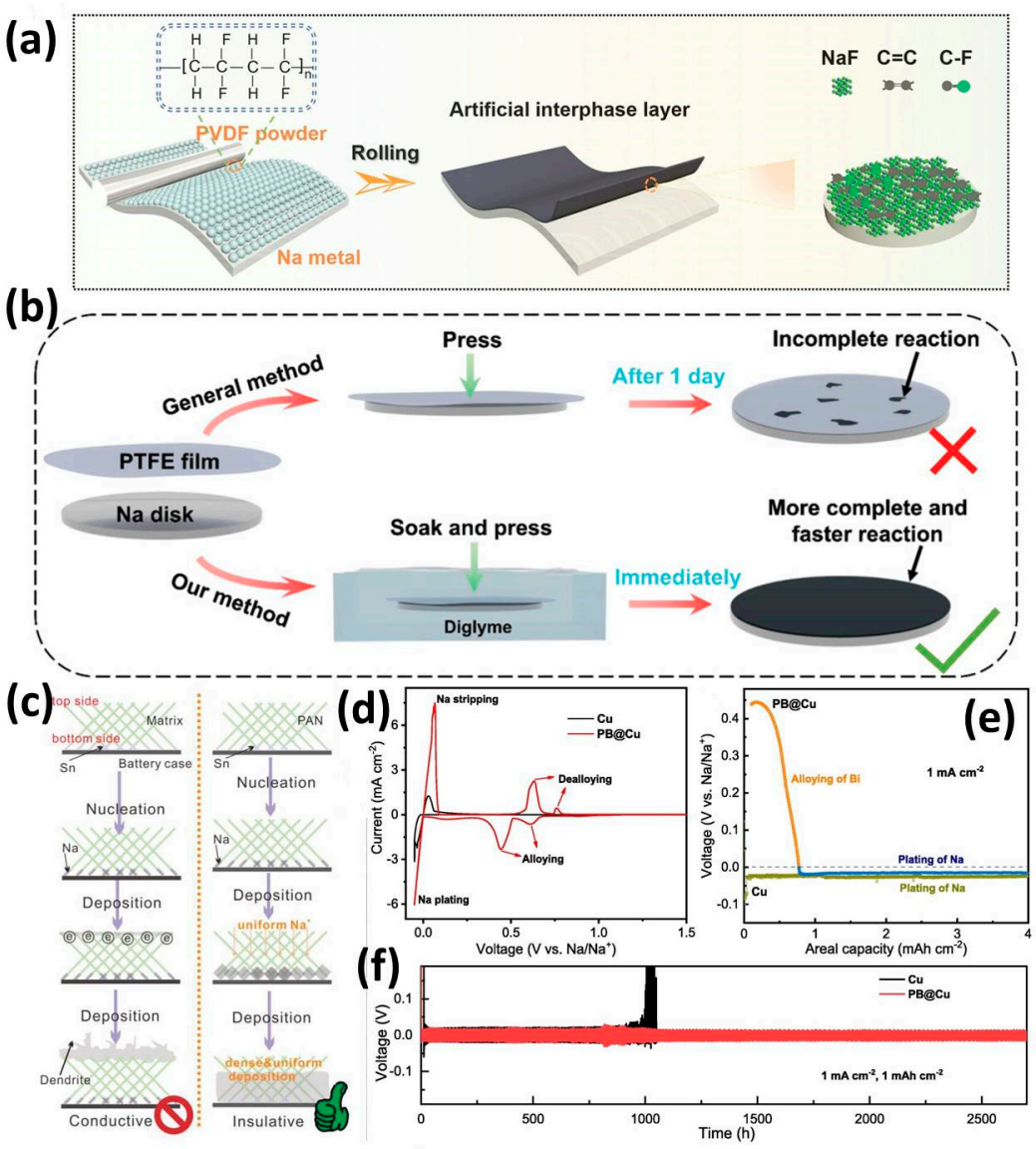

 doi:10.20944/preprints202305.1544.v1

Figure 7. (a) Preparation of PTFE derived hybrid inorganic NaF and organic carbon layers [117]. Copyright 2023, Wiely-VCH. (b) Schematic of pressure and diglyme-induced defluorination reaction for preparing PTFE derived NaF/carbon layer [121]. Copyright 2023, Wiely-VCH. (c) Schematic illustration of PAN-Sn guiding Na deposition with a controlled location and orientation [123]. Copyright 2020, Wiely-VCH. (d) CV curves and (e) the 1st discharge curves of Na||Cu batteries with bare Cu and PB@Cu. (f) Voltage-time curve of Cu and PB@Cu with Na anode at 1 mA cm^{-2} and 1 mAh cm^{-2} [124]. Copyright 2022, Elsevier.

Different from stiff and dense inorganic ALD coatings, the MLD coatings are confirmed to release volume expansion due to the reduced density and increased flexibility of hybrid organic-inorganic layers [90]. Meanwhile, the hybrid layers provide higher tune ability since the integration of organic bonds in MLD coatings provides attractive chemical/electrochemical, mechanical and electrical performances. As expected, the MLD technologies show great improvements for stabilizing Na metal without dendrite growth. As shown in Figure **8**a, in 2017, Zhao et al. used trimethylaluminum and ethylene glycol (Alucone) to introducing an organic-inorganic composite layer on Na anode via MLD at 85 °C. During experimental testing, thickness of 10, 25 and 40 MLD cycles were performed. It is proved that the 25 MLD cycles of AIEG (Na@25Alucone) was optimized for the best. As reported, the SEI on Na@25Alucone showed higher contents of beneficial NaF and Na_2O [125]. The MLD technology is also benefit for solid Na batteries. Lately in 2020, Sun et al. also coating the same Alucone via MLD between Na and solid Na_3SbS_3 and Na_3PS_4 electrolytes as presented in Figure **8**b, in which the Alucone layer work as an interfacial stabilize [126]. As it is confirmed, the type of artificial SEI layer is dependent on the ALD and MLD depositions cycles. If the deposition cycles of ALD and MLD are small, it will form a nano alloy interface; if the deposition cycles of ALD and MLD are large, it will form full monolayers. More recently in 2023, Sun et al. formed nano hybrid interfaces with nano-alloy and nano-laminated structures (from Al_2O_3 to alucone) through ALD deposited inorganic Al_2O_3 and MLD deposited organic alucone for alkali metal anodes in Figure **8**c [127]. By time-of-flight secondary ion mass spectrometry (TOF-SIMS) in Figure **8**d-f, the Na^-, Al^-, CAL^- and AlO^{2-} are probed on the Na surface, which is realized to be robust and chemical/electrochemical stable upon plating/striping. In this study, three types of nano hybrid interfaces are investigated: 1 layer of Al_2O_3 with 1 layer alucone (1ALD-1MLD); 2 layer of Al_2O_3 with 2 layer alucone (2ALD-2MLD) and 5 layer of Al_2O_3 with 5 layer alucone (5ALD-5MLD). At the same time, the total thickness of the nano hybrid interfaces can be controlled by deposited ALD/MLD cycles, mainly including 5, 10 and 25 cycles. For instance, the corresponding samples are donated as (1ALD-1MLD)5; (1ALD-1MLD)10 and (1ALD-1MLD)25. Among all samples, the (1ALD-1MLD)10 alloy interfaces show the best performances at 3 mA cm^{-2}, 1 mAh cm^{-2} for Na metal. The mossy/dendritic Na growth and "dead" Na formation are effectively suppressed, which would account for the improved performance. Finally, the optimal thickness of the Al_2O_3-alucone alloy interface for Na metal is 4 nm.

Preprints (www.preprints.org) | NOT PEER-REVIEWED | Posted: 23 May 2023 doi:10.20944/preprints202305.1544.v1

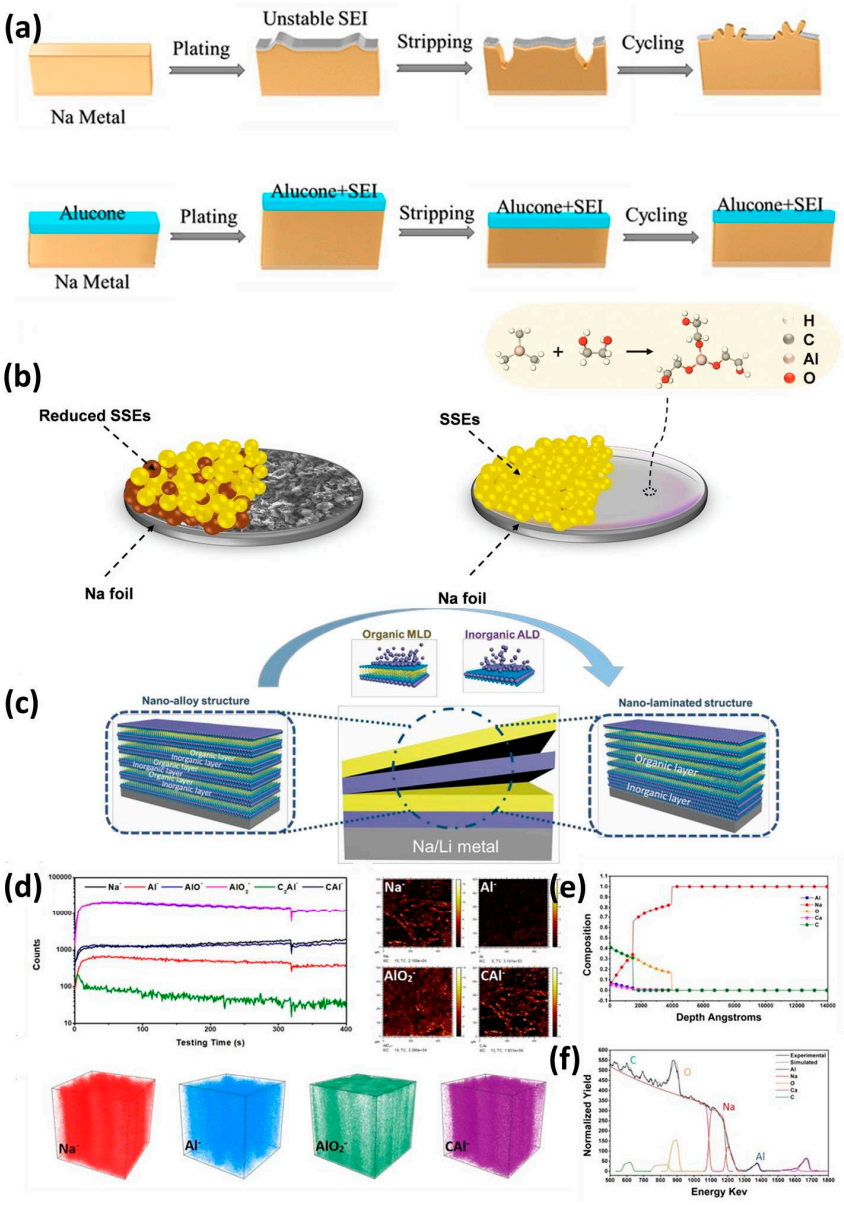

Figure 8. (a) Na plating/striping on bare Na and MLD coated alucone Na [125]. Copyright 2017, American Chemistry Society. (b) Schematic diagram of the interfaces stability of Na and Na@alucone coupled with solid sulfide electrolytes [126]. Copyright 2020, Wiely-VCH. (c) Schematic illustration of the fabrication of the nano-alloy and nano laminated interfacial structures by ALD and MLD deposition. (d) The TOF-SIMS images and depth profiles of Na^-, Al^-, CAL^- and AlO^{2-} ions. (e) The Rutherford backscattering spectrometry and the (f) calculated depth profiles of (1ALD-1MLD)10 alloy interface [127]. Copyright 2023, Wiely-VCH.

4. Conclusions and Perspectives

In this review, we have summarized recent progress on artificial SEI designing for Na metal anodes. The configuration of advanced artificial SEI layers have been proposed by several approaches, including chemical coating, physical deposition, ex-suit conversion reactions and free standing films. On the basis of experimental understanding, the artificial SEI layers can be precisely designed by optimization the composition, thickness and morphology. The protective layer is either highly conductive or mechanical stiffness/flexible. Benefit from these merits, the protective layers are highly effective in regulating uniform Na^+ deposition and suppression dendritic Na formation.

Despite the advantages mentioned above, some deeper challenges still needs to be explored for Na metal: (1) The effect of physical structure, chemical composition, optimization method and Na^+ diffusion mechanism on dendrite suppression should be further investigated; (2) the evolution and failure of artificial SEI during plating/striping need to be studied; (3) Advanced characterization technologies are desired to reveal the inner relationship between SEI and Na metal; (4) The design of SEI should meet the practical conditions especially with limit Na excess and lean electrolyte; (5) the formation/growth of dendritic Na and the dynamic evolution of interphase layer need to be fully understand for better SEI configuration.

In a word, artificial SEI layers with high ionic conductivity, high Young's modulus and mechanical flexible are effective for suppression dendritic Na formation. However, only building artificial SEI is insufficient to solve all the existing issues of Na metal anodes. For these reason, multi-approaches with specific objectives are necessary for promoting the realization of metal Na. We expect this review will promote deeper understanding on the SEI of Na.

Author Contributions: P.C. prepared and revised the raw manuscript. X. W. edited the figures. Y. J. and X. L. revised this manuscript. All authors have read and agreed to the published version of the manuscript.

Funding: This work was supported by the National Natural Science Foundation of China (Nos.52002083) and the start-up grants from Anhui University (No. S020318031/001).

Data Availability Statement: There is no data support for this review.

Conflicts of Interest: The authors declare no competing financial interest.

References

1. Hwang, J. -Y.; Myung, S. -T.; Sun, Y. -K. Sodium-ion batteries: present and future. *Chem. Soc. Rev*. **2017**, *46*, 3529-3614.
2. Abraham, K. M. How Comparable are sodium-ion batteries to lithium-ion counterparts? *ACS Energy Lett*. **2020**, *5*, 3544-3547.
3. Hirsh, H. S.; Li, Y. X.; Tan, D. H. S.; Zhang, M. H.; Zhao, E. Y.; Meng, Y. S. Sodium-ion batteries paving the way for grid energy storage. *Adv. Energy Mater*. **2020**, *10*, 2001274.
4. Liu, T.; Zhang, Y.; Jiang, Z.; Zeng, X.; Ji, J.; Li, Z.; Gao, X.; Sun, M.; Lin, Z.; Ling, M.; Zheng, J. C.; Liang, C. D. Exploring competitive features of stationary sodium ion batteries for electrochemical energy storage. *Energy Environ. Sci*. **2019**, *12*, 1512-1533.
5. Zhao, Y.; Yang, X. F.; Kuo, L. Y. Kaghazchi, P.; Sun, Q.; Liang, J. N.; Wang, B. Q.; Lushington, A.; Li, R. Y.; Zhang, H. M.; Sun, X. L. High capacity, dendrite-free growth, and minimum volume change Na metal anode. *Small* **2018**, *14*, 1703717.
6. Sun, B.; Xiong, P.; Maitra, U.; Langsdorf, D.; Yan, K.; Wang, C. Y.; Janek, J.; Schröder, D.; Wang, G. X. Design strategies to enable the efficient use of sodium metal anodes in high-energy batteries. *Adv. Mater*. **2019**, *32*, 1903891.
7. Cao, R. G.; Mishra, K.; Li, X. L.; Qian, J. F.; Engelhard M. H.; Bowden, M. E.; Han, S. H.; Mueller K. T.; Henderson, W. A.; Zhang, J. -G. Enabling room temperature sodium metal batteries. *Nano Energy* **2016**, *30*, 825-830.
8. Zheng, J. M.; Chen, S. R.; Zhao, W. G.; Song. J. H.; Mueller K. T.; Zhang, J. -G. Extremely stable sodium metal batteries enabled by localized high-concentration electrolytes. *ACS Energy Lett*. **2018**, *3*, 315-321.
9. Lee, Y.; Lee, J.; Lee, J. M.; Kim, K.; Cha, A.; Kang, S. J.; Wi, T.; Kang, S. J.; Lee, H. -W.; Choi, N. -S. Fluoroethylene carbonate-based electrolyte with 1 M sodium bis (fluorosulfonyl) imide enables high-performance sodium metal electrodes. *ACS Appl. Mater. Interfaces* **2018**, *10*, 15270-15280.
10. Ma, B.; Bai, P. Fast charging limits of ideally stable metal anodes in liquid electrolytes. *Adv. Energy Mater*. **2022**, *12*, 2102967.
11. Ji, Y. Y.; Li, J. B.; Li, J. L. Recent development of electrolyte engineering for sodium metal batteries. *Batteries* **2022**, *8*, 157.
12. Zheng, X. Y.; Cao, Z.; Gu, Z. Y.; Huang, L. Q.; Sun, Z. H.; Zhao, T.; Yu, S. J.; Wu, X. L.; Huang, Y. H. Toward high temperature sodium metal batteries via regulating the electrolyte/electrode interfacial chemistries. *ACS Energy Lett*. **2022**, *7*, 2032-2042.
13. Xia, X. M.; Lv, X.; Yao, Y.; Chen, D.; Tang, F.; Liu, N.; Feng, Y. Z.; Rui, X. H.; Yu, Y. A sodiophilic VN interlayer stabilizing a Na metal anode. *Nanoscale Horiz*. **2022**, *7*, 899-907.
14. Shi, H. D.; Yue, M.; Zhang, C. F.; Dong, Y. F.; Lu, P. F.; Zheng, S. H.; Huang, H. J.; Chen, J.; Wen, P. C.; Xu, Z. C.; Zheng, Q.; Li, X. F.; Yu, Y.; Wu, Z. S. 3D flexible, conductive and recyclable $Ti_3C_2T_x$ MXene-melamine foam for high areal capacity and long lifetime alkali-metal anode. *ACS Nano*. **2020**, *14*, 8678.

15. Wang, H.; Bai, W. L.; Wang, H.; Kong, D. Z.; Xu, T. Q.; Zhang, Z. F.; Zang, J. H.; Wang, X. C.; Zhang, S.; Tian, Y. T.; Li, X. J.; Lee, C. S.; Wang, Y. 3D printed Au/rGO microlattice host for dendrite-free sodium metal anode. *Energy Storage Mater.* **2023**, *55*, 631-641.
16. Kang, T.; Sun, C.; Li, Y.; Song, T.; Guan, Z.; Tong, Z.; Nan, J.; Lee, C. S. Dendrite-free sodium metal anodes via solid electrolyte interphase engineering with a covalent organic framework separator. *Adv. Energy Mater.* **2023**, *13*, 2204083.
17. Li, M. H.; Lu, G. J.; Zheng, W. K.; Zhao, Q. N.; Li, Z. P.; Jiang, X. P.; Yang, Z. G.; Li, Z. Y.; Qu, B. H.; Xu, C. H. Multifunctionalized safe separator toward practical sodium-metal batteries with high-performance under high mass loading. *Adv. Funct. Mater.* **2023**, *33*, 2214759.
18. Wang, Y. X.; Dong, H.; Katyal, N.; Hao, H. C.; Liu, P. C.; Celio, H.; Henkelman, G.; Watt, J.; Mitlin, D. Sodium-antimony-telluride intermetallic allows sodium metal cycling at 100% depth of discharge and as anode-free metal battery. *Adv. Mater.* **2022**, *34*, 2106005.
19. Liu, H.; Cheng, X. B.; Huang, J. -Q.; Kaskel, S.; Chou, S. L.; Park, H. S.; Zhang, Q. Alloy anodes for rechargeable alkali-metal batteries: progress and challenge. *ACS Matterials Lett.* **2019**, *1*, 217.
20. Tang, S.; Zhang, Y. Y.; Zhang, X. G.; Li, J. T.; Wang, X. Y.; Yan, J. W.; Wu, D. Y.; Zheng, M. S.; Dong, Q. F.; Mao, B. W. Stable Na plating and stripping electrochemistry promoted by in situ construction of an alloy-based sodiophilic interphase. *Adv. Mater.* **2019**, *31*, 1807495.
21. Wang, H.; Wang, C. L.; Matios, E.; Luo, J. M.; Lu, X.; Zhang, Y. W.; Hu, X. F.; Li, W. Y. Enabling ultrahigh rate and capacity sodium metal anodes with lightweight solid additives. *Energy Storage Mater.* **2020**, *32*, 244-252.
22. Bao, C. Y.; Wang, B.; Liu, P.; Wu, H.; Zhou, Y.; Wang, D. L.; Liu, H. K.; Dou, S. X. Solid electrolyte interphases on sodium metal anodes. *Adv. Funct. Mater.* **2020**, *30*, 2004891.
23. Gao, L.; Chen, J.; Chen, Q. L.; Kong, X. Q. The chemical evolution of solid electrolyte interface in sodium metal batteries. *Sci. Adv.* **2022**, *8*, eabm4606.
24. Wang, T.; Hua, Y. B.; Xu, Z. W.; Yu, J. S. Recent advanced development of artificial interphase engineering for stable sodium metal anodes. *Small* **2022**, *18*, 2102250.
25. Zhao, C. L.; Lu, Y. X.; Yue, J. M.; Pan, D.; Qi, Y. R.; Hu, Y. S.; Chen, L. Q. Advanced Na metal anodes. *J. Energy Chem.* **2018**, *27*, 1584-1596.
26. Li, Z. P.; Zhu, K. J.; Liu, P.; Jiao, L. F. 3D confinement strategy for dendrite-free sodium metal batteries. *Adv. Energy Mater.* **2022**, *12*, 2100359.
27. Chen, X.; Bai, Y. K.; Shen, X.; Peng, H. -J.; Zhang, Q. Sodiophilicity/potassiophilicity chemistry in sodium/potassium metal anodes. *J. Energy Chem.* **2020**, *51*, 1-6.
28. Ma, B. Y.; Lee, Y. J.; Bai, P. Dynamic interfacial stability confirmed by microscopic optical operando experiments enables high-retention-rate anode-free Na metal full cells. *Adv. Sci.* **2021**, *8*, 2005006.
29. Wang, S. Y.; Cai, W. B.; Sun, Z. H.; Huang, F. Y.; Jie, Y. L.; Liu, Y.; Chen, Y. W.; Peng, B.; Cao, R. G.; Zhang, G. Q.; Jiao, S. H. Stable cycling of Na metal anodes in a carbonate electrolyte. *Chem. Commun.* **2019**, *55*, 14375-14378.
30. Mandl, M.; Becherer, J.; Kramer, D.; Mönig, R.; Diemant, T.; Diemant, T.; Behm, J.; Hahn, M.; Böse, O.; Danzer, M. A. Sodium metal anodes: deposition and dissolution behaviour and SEI formation. *Electrochim. Acta* **2020**, *354*, 136698.
31. Lee, B.; Paek, E.; Mitlin, D.; Lee, S. W. Sodium metal anodes: Emerging solutions to dendrite growth. *Chem. Rev.* **2019**, *119*, 5416-5460.
32. Zhao, Y.; Adair, K. R.; Sun, X. L.; Recent developments and insights into the understanding of Na metal anodes for Na-metal batteries. *Energy Environ. Sci.* **2018**, *11*, *2673-2695.*
33. Lei, D. N.; He, Y. B.; Huang, H. J.; Yuan, Y. F.; Zhong, G. M.; Zhao, Q.; Hao, X. G.; Zhang, D. F.; Lai, C.; Zhang, S. W.; Ma, J. B.; Wei, Y. P.; Yu, Q. P.; Lv, W.; Yu, Y.; Li, B. H.; Yang, Q. H.; Yang, Y.; Lu, J.; Kang, F. Y. Cross-linked beta alumina nanowires with compact gel polymer electrolyte coating for ultra-stable sodium metal battery. *Nat. Commun.* **2019**, *10*, 4244.
34. Liu, T. F.; Yang, X, K.; Nai, J. W.; Wang, Y.; Liu, Y. J.; Liu, C. T.; Tao, X. Y. Recent development of Na metal anodes: interphase engineering chemistries determine the electrochemical performance. *Chem. Eng. J.* **2021**, *409*, 127943.
35. Ji, Y. Y.; Sun, H. C.; Li, Z. B.; Ma, L.; Zhang, W. G.; Liu, Y. M.; Pan, L. K. Salt engineering toward stable cation migration of Na metal anodes. *J. Mater. Chem. A* **2022**, *10*, 25539-25545.
36. Liu, W.; Liu, P. C.; Mitlin, D. Review of emerging concepts in SEI analysis and artificial SEI membranes for lithium, sodium, and potassium metal battery anodes. *Adv. Energy Mater.* **2020**, *10*, 2002297.
37. Matios, E.; Wang, H.; Wang, C. L.; Li, W. Y. Enabling safe sodium metal batteries by solid electrolyte interphase engineering: a review. *Ind. Eng. Chem. Res.* **2019**, *58*, 9758-9780.
38. Xia, X. M.; Du, C. F.; Zhong, S. E.; Jiang, Y.; Yu, H.; Sun, W. P.; Pan, H. G.; Rui, X. H., Yu, Y. Homogeneous Na deposition enabling high-energy Na-metal batteries. *Adv. Funct. Mater.* **2022**, *32*, 2110280.
39. Lee, J.; Kim, J.; Kim, S.; Jo, C. S.; Lee, J. A review on recent approaches for designing the SEI layer on sodium metal anodes. *Mater. Adv.* **2020**, *1*, 3143-3166.

40. Liu, W.; Liu, P. C.; Mitlin, D. Tutorial review on structure-dendrite growth relations in metal battery anode supports. *Chem. Soc. Rev*. **2020**, *49*, 7284-7300.
41. Lin, Z.; Liu, T. F.; Ai, X. P.; Liang, C. D. Aligning academia and industry for unified battery performance metrics. *Nat. Commun*. **2018**, *9*, 5262.
42. Lee, K.; Lee, Y. J.; Lee, M. J.; Han, J. H.; Lim, J.; Ryu, K.; Yoon, H.; Kim, B. H.; Kim, B. J.; Lee, S. W. A 3D hierarchical host with enhanced sodiophilicity enabling anode-free sodium-metal batteries. *Adv. Mater.* **2022**, *34*, 2109767.
43. Yang, W.; Yang, W.; Dong, L. B.; Shao, G. J.; Wang, G. X.; Peng, X. W. Hierarchical ZnO nanorod arrays grown on copper foam as an advanced three-dimensional skeleton for dendrite-free sodium metal anodes. *Nano Energy* **2021**, *80*, 105563.
44. Wang, C. L.; Wang, H.; Matios, E.; Hu, X. F.; Li, W. Y. A chemically engineered porous copper matrix with cylindrical core-shell skeleton as a stable host for metallic sodium anodes. *Adv. Funct. Mater.* **2018**, *28*, 1802282.
45. Ma, Y.; Gu, Y. T.; Yao, Y. Z.; Jin, H. D.; Zhao, X. H.; Yuan, X. T.; Lian, Y. L.; Qi, P. W.; Shah, R.; Peng, Y.; Deng, Z. Alkaliphilic Cu_2O nanowires on copper foam for hosting Li/Na as ultrastable alkali-metal anodes. *J. Mate. Chem. A* **2019**, *7*, 20926-20935.
46. Mubarak, N.; Ihsan-Ul-Haq, M.; Huang, H.; Cui, J.; Yao, S. S.; Susca, A.; Wu, J. X.; Wang, M. Y.; Zhang, X. H.; Huang, B. L.; Kim, J. K. Metal organic framework-induced mesoporous carbon nanofibers as ultrastable Na metal anode host. *J. Mate. Chem. A* **2020**, *8*, 10269-10282.
47. Yue, L.; Qi, Y. R.; Niu, Y. B.; Bao, S. J.; Xu, M. W. Low-barrier, dendrite-free, and stable Na plating/stripping enabled by gradient sodiophilic carbon skeleton. *Adv. Energy Mater.* **2021**, *11*, 2102497.
48. Wang, Z. X.; Huang, Z. X.; Wang, H.; Li, W. D.; Wang, B. Y.; Xu, J. M.; Xu, T. T.; Zang, J. H.; Kong, D. Z.; Li, X. J.; Yang, H. Y.; Wang, Y. 3D-printed sodiophilic V_2CT_x/rGO-CNT MXene microgrid aerogel for stable Na metal anode with high areal capacity. *ACS. Nano.* **2022**, *16*, 9105-9116.
49. Shi, H. D.; Yue, M.; John Zhang, C. F.; Dong, Y. F.; Liu, P. F.; Zheng, S. H.; Huang, H. J.; Chen, J.; Wen, P. C.; Xu, Z. C.; Zheng, Q.; Li, X. F.; Yu, Y.; Wu, Z. -S. 3D flexible, conductive, and recyclable $Ti_3C_2T_x$ MXene-melamine foam for high-areal-capacity and long-lifetime alkali-metal anode. *ACS Nano* **2020**, *14*, 8678-8688.
50. Chu, C. X.; Li, R.; Cai, F. P.; Bai, Z. C.; Wang, Y. X.; Xu, X.; Wang, N.; Yang, J.; Dou, S. X. Recent advanced skeletons in sodium metal anodes. *Energy Environ. Sci.* **2021**, *14*, 4318-4340.
51. Yang, C.; Xin, S.; Mai, L. Q.; You, Y. Materials design for high-safety sodium-ion battery. *Adv. Energy Mater.* **2021**, *11*, 2000974.
52. Wang, H.; Yu, D.; Kuang, C.; Cheng, L.; Li, W.; Feng, X.; Zhang, Z.; Zhang, X.; Zhang, Y. Alkali metal anodes for rechargeable batteries. *Chem.* **2019**, *5*, 313-338.
53. Zhang, X. Q.; Cheng X. B.; Zhang, Q. Advances in interfaces between Li metal anode and electrolyte. *Adv. Mater. Interfaces* **2018**, *5*, 1701097.
54. Xu, Z. X.; Yang, J.; Zhang, T.; Sun, L. M.; Nuli, Y. N.; Wang, J. L.; Hirano, S. Stable Na metal anode enabled by a reinforced multistructural SEI layer. *Adv. Funct. Mater*. **2019**, *29*, 1901924.
55. Fang, W.; Jiang, H.; Zheng, Y.; Zheng, H.; Liang, X.; Chen, C. H.; Xiang, H. F. A bilayer interface formed in high concentration electrolyte with SbF_3 additive for long-cycle and high-rate sodium metal battery. *J. Power Sources* **2020**, *455*, 227956.
56. Wang, G.; Xiong, X. H.; Xie, D.; Fu, X. X.; Lin, Z. H.; Yang, C. H.; Zhang, K. L.; Liu, M. L. A scalable approach for dendrite-free alkali metal anodes via room-temperature facile surface fluorination. *ACS Appl. Mater. Interfaces* **2019**, *11*, 4962-4968.
57. Zhou, X. F.; Liu, F. F.; Wang, Y. J.; Yao, Y.; Shao, Y.; Rui, X. H.; Wu, F. X.; Yu, Y. Heterogeneous interfacial layers derived from the in situ reaction of CoF_2 nanoparticles with sodium metal for dendrite-free Na metal anodes. *Adv. Energy Mater.* **2022**, *12*, 2202323.
58. Miao, X. G.; Di, H. X.; Ge, X. L.; Zhao, D. Y.; Wang, P.; Wang, R. T.; Wang, C. X.; Yin, L. W. AlF_3-modified anode-electrolyte interface for effective Na dendrites restriction in NASICON-based solid-state electrolyte. *Energy Storage Mater.* **2020**, *30*, 170-178.
59. Cheng, Y. F.; Yang, X. M.; Li, M. H.; Li, X. Y.; Lu, X. Z.; Wu, D. J.; Han, B.; Zhang, Q.; Zhu, Y. M.; Gu, M. Enabling ultrastable alkali metal anodes by artificial solid electrolyte interphase fluorination. *Nano Lett.* **2022**, *22*, 4347-4353.
60. Xie, Y. Y.; Hu, J. X.; Zhang, L. Y.; Wang, A. N.; Zheng, J. Q.; Li, H. X.; Lai, Y. Q.; Zhang, Z. A. Stabilizing Na metal anode with NaF interface on spent cathode carbon from aluminum electrolysis. *Chem. Commun.* **2021**, *57*, 7561-7564.
61. Zheng, X. Y.; Fu, H. Y.; Hu, C. C.; Xu, H.; Huang, Y.; Wen, J. Y.; Sun, H. B.; Luo, W.; Huang, Y. H. Toward a stable sodium metal anode in carbonate electrolyte: a compact, inorganic alloy interface. *J. Phys. Chem. Lett*. **2019**, *10*, 707-714.
62. Kumar, V.; Eng, A. Y. S.; Wang, Y.; Nguyen, D. T.; Ng, M. F.; Seh, Z. W. An artificial metal-alloy interphase for high-rate and long-life sodium-sulfur batteries. *Energy Storage Mater.* **2020**, *19*, 1-8.

63. Lu, Q. Q.; Omar, A.; Hantusch, M.; Oswald, S.; Ding, L.; Nielsch, K.; Mikhailova, D. Dendrite-free and corrosion-resistant sodium metal anode for enhanced sodium batteries. *Appl. Surf. Sci.* **2022**, *600*, 154168.
64. Chen, Q. W.; He, H.; Hou, Z.; Zhuang, W. M.; Zhang, T. X.; Sun, Z. Z.; Huang, L. M. Building an artificial solid electrolyte interphase with high-uniformity and fast ion diffusion for ultralong-life sodium metal anodes. *J. Mate. Chem. A* **2020**, *8*, 16232-16237.
65. Tian, H. J.; Shao, H. Z.; Chen, Y.; Fang, X. Q.; Xiong, P.; Sun, B.; Nottenc, P. H. L.; Wang, G. X. Ultra-stable sodium metal-iodine batteries enabled by an in-situ solid electrolyte interphase. *Nano Energy* **2019**, *57*, 692-702.
66. Choudhury, S.; Wei, S. Y.; Ozhabes, Y.; Gunceler, D.; Zachman, M. J.; Tu, Z. Y.; Shin, J. H.; Nath, P.; Agrawall, A.; Kourkoutis, L. F.; Arias, T. A.; Archer, L. A. Designing solid-liquid interphases for sodium batteries. *Nat. Commun.* **2017**, *8*, 898.
67. Zhao, Y.; Liang, J. W.; Sun, Q.; Goncharova, L. V.; Wang, J. W.; Wang, C. H.; Adair, K. R.; Li, X. N.; Zhao, F. P.; Sun, Y. P.; Li, R. Y.; Sun, X. L. In-situ formation of highly controllable and stable Na_3PS_4 as protective layer for Na metal anode. *J. Mate. Chem. A* **2019**, *47*, 4119-4125.
68. Lu, K.; Gao, S. Y.; Li, G. S.; Kaelin, J.; Zhang, Z. C.; Cheng, Y. W. Regulating interfacial Na-ion flux via artificial layers with fast ionic conductivity for stable and high-rate Na metal batteries. *ACS Materials Lett*. **2019**, *1*, 303-309.
69. Zhang, D.; Li, B.; Wang, S.; Yang, S. B. Simultaneous formation of artificial SEI film and 3D host for stable metallic sodium anodes. *ACS Appl. Mater. Interfaces* **2017**, *9*, 40265-40272.
70. Wang, X. C.; Fu, L.; Zhan, R. M.; Wang, L. Y.; Li, G. C.; Wan, M. T.; Wu, X. L.; Seh, Z. W.; Wang, L.; Sun, Y. M. Addressing the low solubility of a solid electrolyte interphase stabilizer in an electrolyte by composite battery anode design. *ACS Appl. Mater. Interfaces* **2021**, *13*, 13354-13361.
71. Shi, P. C.; Zhang, S. P.; Lu, G. X.; Wang, L. F.; Jiang, Y.; Liu, F. F.; Yao, Y.; Yang, H.; Ma, M. Z.; Ye, S. F.; Tao, X. Y.; Feng, Y. Z.; Wu, X. J.; Rui, X. H.; Yu, Y. Red phosphorous-derived protective layers with high ionic conductivity and mechanical strength on dendritefree sodium and potassium metal anodes. *Adv. Energy Mater*. **2021**, *11*, 2003381.
72. Yang, H.; He, F. X.; Li, M. H.; Huang, F. Y.; Chen, Z. H.; Shi, P. C.; Liu, F. F.; Jiang, Y.; He, L. X.; Gu, M.; Yu, Y. Design principles of sodium/potassium protection layer for high-power high-energy sodium/potassium-metal batteries in carbonate electrolytes: a case study of Na_2Te/K_2Te. *Adv. Mater.* **2021**, *33*, 2106353.
73. Luo, Z.; Tao, S. S.; Tian, Y.; Xu, L. Q.; Wang, Y.; Cao, X. Y.; Wang, Y. P.; Deng, W. T.; Zou, G. Q.; Liu, H.; Hou, H. S.; Ji, X. B. Robust artificial interlayer for columnar sodium metal anode. *Nano Energy* **2022**, *97*, 107203.
74. Zhang, Y. J.; Huang, Z. Y.; Liu, H. X.; Chen, H. F.; Wang, Y. Y.; Wu, K.; Wang, G. Y.; Wu, C. Amorphous phosphatized hybrid interfacial layer for dendrite-free sodium deposition. *J. Power Sources* **2023**, *569*, 233023.
75. Jiang, Y.; Yang, Y.; Ling, F. X.; Lu, G. X.; Huang, F. Y.; Tao, X. Y.; Wu, S. F.; Cheng, X. L.; Liu, F. F.; Li, D. J.; Yang, H.; Yao, Y.; Shi, P. C.; Chen, Q. W.; Rui, X. H.; Yu, Y. Artificial heterogeneous interphase layer with boosted ion affinity and diffusion for Na/K-metal batteries. *Adv. Mater.* **2022**, *34*, 2109439.
76. Xia, X. M.; Xu, S. T.; Tang, F.; Yao, Y.; Wang, L. F.; Liu, L.; He, S. N.; Yang, Y. X.; Sun, W. P.; Xu, C.; Feng, Y. Z.; Pan, H. G.; Rui, X. H.; Yu, Y. A multifunctional interphase layer enabling superior sodium-metal batteries under ambient temperature and -40°C. *Adv. Mater.* **2023**, *35*, 2209511.
77. Xia, X. M.; Yang, Y.; Chen, K. Z.; Xu, S. T.; Tang, F.; Liu, L.; Xu, C.; Rui, X. H. Enhancing interfacial strength and wettability for wide-temperature sodium metal batteries. *Small*. **2023**, *19*, 2300907.
78. Li, D. J.; Sun, Y. J.; Li, M. H.; Cheng, X. L.; Yao, Y.; Huang, F. Y.; Jiao, S. H.; Gu, M.; Rui, X. H.; Ali, Z.; Ma, C.; Wu, Z. -S. Yu, Y. Rational design of an artificial SEI: alloy/solid electrolyte hybrid layer for a highly reversible Na and K metal anode. *ACS Nano.* **2022**, *16*, 16966-16975.
79. Chu, F. L.; Hu, J. L.; Tian, J.; Zhou, X. J.; Li, Z.; Li, C. L. In situ plating of porous Mg network layer to reinforce anode dendrite suppression in Li-metal batteries. *ACS Appl. Mater. Interfaces* **2018**, *10*, 12678-12689.
80. Tu, Z. Y.; Choudhury, S.; Zachman, M. J.; Wei, S. Y.; Zhang, K. H.; Kourkoutis, L. F.; Archer, L. A. Fast ion transport at solid-solid interfaces in hybrid battery anodes. *Nature Energy* **2018**, *3*, 310-316.
81. Ma, M. Y.; Lu, Y.; Yan, Z. H.; Chen, J. In situ synthesis of Bi layer on Na metal anode for fast nterfacial transport in $Na-O_2$ batteries. *Batteries & Supercaps* **2019**, **2**, 663-667.
82. Peng, Z.; Song, J. H.; Huai, L. Y.; Jia, H. P.; Xiao, B. W.; Zou, L. F.; Zhu, G. M.; Martinez, A.; Roy, S.; Murugesan, V.; Lee, H.; Ren, X. D.; Li, Q. Y.; Liu, B.; Li, X. L.; Wang, D. Y.; Wu, X.; Zhang, J. G. Enhanced stability of Li metal anodes by synergetic control of nucleation and the solid electrolyte interphase. *Adv. Energy Mater.* **2019**, *9*, 1901764.
83. Liu, Y.; Li, Q. Z.; Lei, Y. Y.; Zhou, D. L.; Wu, W. W.; Wu, X. H. Stabilizing sodium metal anode by in-situ formed Ag metal layer. *J. Alloy Compd.* **2022**, *926*, 166850.
84. Liu, C. Y.; Xie, Y. Y.; Li, H. X.; Xu, J. Y.; Zhang, Z. A. In situ construction of sodiophilic alloy interface enabled homogenous Na nucleation and deposition for sodium metal anode. *J. Electrochem. Soc*. **2022**, *169*, 080521.
85. Lv, X.; Tang, F.; Yao, Y.; Xu, C.; Chen, D.; Liu, L.; Feng, Y. Z.; Rui, X. H.; Yu, Y. Sodium-gallium alloy layer for fast and reversible sodium deposition. *SusMat* **2022**, *2*, 699-707.

86. Li, G. C.; Yang, Q. P.; Chao, J.; Zhang, B.; Wan, M. T.; Liu, X. X.; Mao, E.; Wang, L.; Yang, H.; Seh, Z. W.; Jiang, J. J.; Sun, Y. M. Enhanced processability and electrochemical cyclability of metallic sodium at elevated temperature using sodium alloy composite. *Energy Storage Mater.* **2021**, *35*, 310-316.
87. Luo, W.; Lin, C. -F.; Zhao, O.; Noked, M.; Zhang, Y.; Rubloff, G. W.; Hu, L. B. Ultrathin surface coating enables the stable sodium metal anode. *Adv. Energy Mater.* **2017**, *7*, 1601526.
88. Zhao, Y.; Goncharova, L. V.; Lushington, A.; Sun, Q.; Yadegari, H.; Wang, B. Q.; Xiao, W.; Li, R. Y.; Sun, X. L. Superior stable and long life sodium metal anodes achieved by atomic layer deposition. *Adv. Mater*. **2017**, *29*, 1606663.
89. Jin, E.; Tantratian, K.; Zhao, C.; Codirenzi, A.; Goncharova, L. V.; Wang, C. H.; Yang, F. P.; Wang, Y. J.; Pirayesh, P.; Guo, J. H.; Chen, L.; Sun, X. L.; Zhao, Y. Ionic conductive and highly-stable interface for alkali metal anodes. *Small* **2022**, *18*, 2203045.
90. Sullivan, M.; Tang, P.; Meng, X. B. Atomic and molecular layer deposition as surface engineering techniques for emerging alkali metal rechargeable batteries. *Molecules* **2022**, *27*, 6170.
91. Ye, L.; Liao, M.; Zhao, T. C.; Sun, H.; Zhao, Y.; Sun, X. M.; Wang, B. J.; Peng, H. S. A sodiophilic interphase-mediated, dendrite-free anode with ultrahigh specific capacity for sodium-metal batteries. *Angew. Chem. Int. Ed*. **2019**, *131*, 2-9.
92. Liu, P.; Yi, H. T.; Zheng, S. Y.; Li, Z. P.; Zhu, K. J.; Sun, Z. Q.; Jin, T.; Jiao, L. F. Regulating deposition behavior of sodium ions for dendrite-free sodium-metal anode. *Adv. Energy Mater.* **2021**, *11*, 2101976.
93. Zhang, S. J.; You, J. H.; He, Z. W.; Zhong, J. J.; Zhang, P. F.; Yin, Z. W.; Pan, F.; Ling, M.; Zhang, B. K.; Lin, Z. Scalable lithiophilic/sodiophilic porous buffer layer fabrication enables uniform nucleation and growth for lithium/sodium metal batteries. *Adv. Funct. Mater.* **2022**, *32*, 2200967.
94. Wang, H.; Wang, C. L.; Matios, E.; Li, W. Y.; Critical role of ultrathin graphene films with tunable thickness in enabling highly stable sodium metal anodes. *Nano Lett*. **2017**, *17*, 6808-6815.
95. Tian, H. Z.; Seh, Z. W.; Yan, K.; Fu, Z. H.; Tang, P.; Lu, Y. Y.; Zhang, R. F.; Legut, D.; Cui, Y.; Zhang, Q. F. Theoretical investigation of 2D layered materials as protective films for lithium and sodium metal anodes. *Adv. Energy Mater.* 2017, *7*, *1602528*.
96. He, X.; Jin, S.; Miao, L. C.; Cai, Y. C.; Hou, Y. P.; Li, H. X.; Zhang, K.; Yan, Z. H.; Chen, J. A 3D hydroxylated MXene/carbon nanotubes composite as a scaffold for dendrite-free sodium-metal Electrodes. *Angew Chem. Int. Ed.* **2020**, *59*, 16705-16711.
97. Luo, J. M.; Wang, C. L.; Wang, H.; Hu, X. F.; Matios, E.; Lu, X.; Zhang, W. K.; Tao, X. Y.; Li, W. Y. Pillared MXene with ultralarge interlayer spacing as a stable matrix for high performance sodium metal anodes. *Adv. Funct. Mater.* **2019**, *29*, 1805946.
98. Jiang, H. Y.; Lin, X. H.; Wei, C. L.; Zhang, Y. C.; Feng, J. K.; Tian, X. L. Sodiophilic Mg^{2+}-decorated Ti_3C_2 MXene for dendrite-free sodium metal batteries with carbonate-based electrolytes. *Small* **2022**, *18*, 2107637.
99. Bao, C. Y.; Wang, J. H.; Wang, B.; Sun, J. G.; He, L. C.; Pan, Z. H.; Jiang, Y. P.; Wang, D. L.; Liu, X. M.; Dou, S. X.; Wang, J. 3D sodiophilic Ti_3C_2 MXene@g-C_3N_4 hetero-interphase raises the stability of sodium metal anodes. *ACS Nano* **2022**, *16*, 17197-17209.
100. Shi, R. J.; Shen, Z.; Yue, Q. Q.; Zhao, Y. Advances in functional organic material-based interfacial engineering on metal anodes for rechargeable secondary batteries. *Nanoscale*. **2023**, *doi: 10.1039/d3nr01306e*.
101. Li, N. W.; Shi, Y.; Yin, Y. X.; Zeng, X. X.; Li, J. Y.; Li, C. J.; Wan, L. J.; Wen, R.; Guo, Y. G. A flexible solid electrolyte interphase layer for long-life lithium metal anodes. *Angew Chem. Int. Ed*. **2018**, *130*, 1521-1525.
102. Ma, J. L.; Yin, Y. B.; Liu, T.; Zhang, X. B.; Yan, J. M.; Jiang, Q. Suppressing sodium dendrites by multifunctional polyvinylidene fluoride (PVDF) interlayers with nonthrough pores and high flux/affinity of sodium ions toward long cycle life sodium oxygen-batteries. *Adv. Funct. Mater.* **2018**, *28*, 1703931.
103. Hou, Z.; Wang, W. H.; Yu, Y. K.; Zhao, X. X.; Chen, Q. W.; Zhao, L. F.; Di, Q.; Ju, H. X.; Quan, Z. W. Poly(vinylidene difluoride) coating on Cu current collector for high-performance Na metal anode. *Energy Storage Mater*. **2020**, *24*, 588-593.
104. Shuai, Y.; Lou, J.; Pei, X. L.; Su, C. Q.; Ye, X. S.; Zhang, L. M.; Wang, Y.; Xu, Z. X.; Gao, P. P.; He, S. J.; Wang, Z. L.; Chen, K, H. Constructing an in situ polymer electrolyte and a Na-rich artificial SEI layer toward practical solid-state Na metal batteries. *ACS Appl. Mater. Interfaces* **2022**, **14**, 45382-45391.
105. Lu, Q. Q.; Omar, A.; Ding, L.; Oswald, S.; Hantusch, M.; Giebeler, L.; Nielsch, K.; Mikhailova, D. A facile method to stabilize sodium metal anodes towards high-performance sodium batteries. *J. Mater. Chem. A* **2021**, *9*, 9038-9047.
106. Wei, S. Y.; Choudhury, S.; Xu, J.; Nath, P.; Tu, Z. Y.; Archer, L. A. Highly stable sodium batteries enabled by functional ionic polymer membranes. *Adv. Mater*. **2017**, *29*, 1605512.
107. Zhu, M.; Wang, G, Y.; Liu, X.; Guo, B. K.; Xu, G.; Huang, Z. Y.; Wu, M. H.; Liu, H, K.; Dou, S. X.; Wu, C. Dendrite-free sodium metal anodes enabled by a sodium benzenedithiolate-rich protection layer. *Angew Chem. Int. Ed.* **2020**, *132*, 6658-6662.
108. Wang, C. Z.; Zheng, Y.; Chen, Z. N.; Zhang, R. R.; He, W.; Li, K. X.; Yan, S.; Cui, J. Q.; Fang, X. L.; Yan, J. W.; Xu, G.; Peng, D. L.; Ren, B.; Zheng, N. F.; Robust anode-free sodium metal batteries enabled by artificial sodium formate interface. *Adv. Energy Mater.* **2023**, *13*, 2204125.

109. Qian, J.; Li, Y.; Zhang, M. L.; Luo, R.; Wang, F. J.; Ye, Y. S.; Xing, Y.; Li, W. L.; Qu, W. J.; Wang, L. L.; Li, L.; Li, Y. J.; Wu, F.; Chen, R. J. Protecting lithium/sodium metal anode with metal-organic framework based compact and robust shield. *Nano Energy* **2019**, *60*, 866-874.
110. Zhu, M. Q.; Li, S. M.; Li, B.; Gong, Y. J.; Du, Z. G.; Yang, S. B. Homogeneous guiding deposition of sodium through main group II metals toward dendrite-free sodium anodes. *Sci. Adv.* 2019, 5, eaau6264.
111. Miao, X. G.; Wang, P.; Sun, R.; Li, J. F.; Wang, Z. X.; Zhang, T.; Wang, R. T.; Li, Z. Q.; Bai, Y. J.; Hao, R.; Yin, L. W. Liquid metal-organic frameworks in-situ derived interlayer for high-performance solid-state Na-metal batteries. *Adv. Energy Mater.* **2021**, *11*, 2102396.
112. Hu, Y. Y.; Han, R. X.; Mei, L.; Liu, J. L.; Sun, J. C.; Yang, K.; Zhao, J. W. Design principles of MOF-related materials for highly stable metal anodes in secondary metal-based batteries. *Mater. Today Energy 2021*, *19*, 100608.
113. He, Y. B.; Qiao, Y.; Chang, Z.; Zhou, H. S. The potential of electrolyte filled MOF membranes as ionic sieves in rechargeable batteries. *Energy Environ. Sci. 2019*, *12*, 2327-2344.
114. Kim, Y. J.; Lee, H.; Noh, H.; Lee, J.; Kim, S.; Ryou, M. H.; Lee, Y. M.; Kim, H. T. Enhancing the cycling stability of sodium metal electrode by building an inorganic/organic composite protective layer. *ACS Appl. Mater. Interfaces* **2017**, *9*, 6000-6006.
115. Wang, S. Y.; Jie, Y. L.; Sun, Z. H.; Cai, W. B.; Chen, Y. W.; Huang, F. Y.; Liu, Y.; Li, X. P.; Du, R. Q.; Cao, R. G.; Zhang, G. Q.; Jiao, S. H. An implantable artificial protective layer enables stable sodium metal anodes. *ACS Appl. Energy Mater.* **2020**, *3*, 8688-8694.
116. Hou, Z.; Wang, W. H.; Chen, Q. W.; Yu, Y. K.; Zhao, X. X.; Tang, M.; Zheng, Y. Y.; Quan, Z. W. Hybrid protective layer for stable sodium metal anodes at high utilization. *ACS Appl. Mater. Interfaces* **2019**, *11*, 37693-37700.
117. Lv, X.; Tang, F.; Xu, S. T.; Yao, Y.; Yuan, Z. S.; Liu, L.; He, S. N.; Yang, Y. X.; Sun, W. P.; Pan, H. G.; Rui, X. H.; Yu, Y. Construction of inorganic/organic hybrid layer for stable Na metal anode operated under wide temperatures. *Small* **2023**, *19*, 2300215.
118. Xie, Y. Y.; Liu, C. Y.; Zheng, J. Q.; Li, H. X.; Zhang, L. Y.; Zhang, Z. A. NaF-rich protective layer on PTFE coating microcrystalline graphite for highly stable Na metal anodes. *Nano Res. 2023*, *16*, 2436-2444.
119. Xu, M. Y.; Li, Y.; Ihsan-Ul-Haq, M.; Mubarak, N.; Liu, Z. J.; Wu, J. X.; Luo, Z. T.; Kim, J. K. NaF-rich solid electrolyte interphase for dendrite-free sodium metal batteries. *Energy Storage Mater.* **2022**, *44*, 477-486.
120. Tai, Z. X.; Liu, Y. J.; Yu, Z. P.; Lu, Z. Y.; Bondarchuk, O.; Peng, Z. J.; Liu, L. F. Non-collapsing 3D solid-electrolyte interphase for high-rate rechargeable sodium metal batteries. *Nano Energy* **2022**, *94*, 106947.
121. Zhang, W.; Yang, X. K.; Wang, J. C.; Zheng, J. L.; Yue, K.; Liu, T. F.; Wang, Y.; Nai, J. W.; Liu, Y. J.; Tao, X. Y. Rapidly constructing sodium fluoride-rich interface by pressure and diglyme-induced defluorination reaction for stable sodium metal anode. *Small* **2023**, *19*, 2207540.
122. Chen, Q. W.; Hou, Z.; Sun, Z. Z.; Pu, Y. Y.; Jiang, Y. B.; Zhao, Y.; He, H.; Zhang, T. X.; Huang, L. M. Polymer-inorganic composite protective layer for stable Na metal anodes. *ACS Appl. Energy Mater.* **2020**, *3*, 2900-2906.
123. Xu, Y.; Wang, C. L.; Matios, E.; Luo, J. M.; Hu, X. F.; Yue, Q.; Kang, Y. J.; Li, W. Y. Sodium deposition with a controlled location and orientation for dendrite-free sodium metal batteries. *Adv. Energy Mater.* **2020**, *10*, 2002308.
124. Zhang, J. L.; Wang, S.; Wang, W. H.; Li, B. H. Stabilizing sodium metal anode through facile construction of organic-metal interface. *J. Energy Chem.* **2022**, *66*, 133-139.
125. Zhao, Y.; Goncharova, L. V.; Zhang, Q.; Kaghazchi, P.; Sun, Q.; Lushington, A.; Wang, B. Q.; Li, R. Y.; Sun, X. L. Inorganic-organic coating via molecular layer deposition enables long life sodium metal anode. *Nano Lett.* **2017**, *17*, 5653-5659.
126. Zhang, S. M.; Zhao, Y.; Zhao, F. P.; Zhang, L.; Wang, C. H.; Li, X. N.; Liang, J. W.; Li, W. H.; Sun, Q.; Yu, C.; Luo, J.; Doyle-Davis, K.; Li, R. Y.; Sham, T. K.; Sun, X. L. Gradiently sodiated alucone as an interfacial stabilizing strategy for solid-state Na metal batteries. *Adv. Funct. Mater.* **2020**, *30*, 2001118.
127. Pirayesh, P.; Tantratian, K.; Amirmaleki, M.; Yang, F. P.; Jin, E. Z.; Wang, Y. J.; Goncharova, L. V.; Guo, J. H.; Filleter, T.; Chen, L.; Zhao, Y. From nano-alloy to nano-laminated interfaces for highly stable alkali metal anodes. *Adv. Mater.* **2023**, *35*, 2301414.